Contactor Fault Detection and Classification System Using Optical Fiber Bragg Grating Sensors

Eduardo H. Dureck, Daniel Benetti, Wiston C. P. Junior, Thiago H. Silva, Heitor S. Lopes, Uilian J. Dreyer, Kleiton M. Sousa, Daniel R. Pipa and Jean Carlos Cardozo da Silva

***Abstract*— Electrical switching devices control and protect systems at various voltages. Monitoring them ensures safety and reliability. This study introduces a method to instrument and analyze these devices, using ABB AX40 AC contactors and Fiber Bragg Grating (FBG) sensors. The dynamic strain sensing of the FBG was used for acquiring signals for the analysis of the switching event. The devices were subjected to three simulated fault conditions: the inner contact blockage, pressure spring wear-off, and load contact wear-off. For recognizing the degradation patterns of the mechanisms, the data acquired during the switching events were submitted to several steps, such as data augmentation, feature selection, and classification. With a Support Vector Machine as the classifier, a score of 80% for fault detection in training and validation was achieved. Within this detection, a score of 80.2% for fault classification was achieved. Regarding the repeatability test data set, it was able to achieve results of fault detection of 72.1% and within this detection, a score of 85% for fault classification was achieved. We also used both, the CN2 Rule classifier and the Decision Tree classifier, to extract human-comprehensible information from the frequency spectrum features. The results presented in this paper suggest the suitability of FBG and machine learning methods for the predictive maintenance of switching devices and the importance of repeatability for future field applications.**

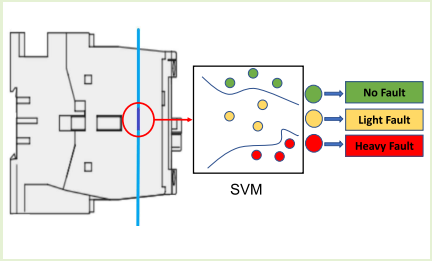

***Index Terms*— Contactors, fiber Bragg grating, fault detection, support vector machine, feature selection**

I. Introduction

SWITCHING devices are essential elements of electrical systems, mainly in the industrial and distribution areas. Although electromechanical switching equipments have an estimated lifespan, they might malfunction before the predicted end of life. Such a problem may lead to profit losses, fatal accidents, and a drop in electric distribution quality. Some of the main reasons for malfunctions are the carbon deposit obstructing the inner contacts [1], core or contact blockage, voltage sag, and contact bounce [2]. To ensure the optimal operation of those equipments, sensors can be used to monitor their condition.

Measurement systems for monitoring vibration pattern signals during a switching event are already in use in equipments, such as On Load Tap Changers (OLTC) transformers and circuit breakers [3], [4]. Most of these systems use electrical accelerometers for measuring vibrations. Usually, such sensors are non-invasive, and data collected from them are analyzed in the time domain or time-frequency domain so that the switching conditions can be inferred [5].The common electronic sensors, however, are prone to interference from electromagnetic sources prevalent in these installations [6]. Hence, fiber optic sensors such as Fiber Bragg Grating (FBG) emerge as a superior alternative, offering immunity to electromagnetic disturbances and durability in harsh environments, such as marine settings. This makes FBGs an increasingly attractive choice for implementation in various electrical circuits and equipment, extending their utility beyond traditional applications [7]–[9].

An FBG is a periodic modulation of the refractive index of the optical fiber core that reflects part of the incident light spectrum. This reflection band is centered at the Bragg wavelength and its value is susceptible to mechanical deformations and temperature changes [10], [11].

The FBGs, in general, have proven their effectiveness in several applications of modern electrical machines. They become a highly attractive component to be used as a sensor element in the environment of electrical circuits [12]. However, their use in switching equipment is of recent application. Some previous papers address applications for classifying different

Manuscript Received 19 October, 2023; revised 27 November, 2023; accepted 19 December, 2023; Date of publication XXXXXXX; date of current version XXXXXXXX. This work was supported in part by the Coordination of Superior Level Staff Improvement (CAPES), in part by the National Council for Scientific and Technological Development (CNPq), in part by Funding Authority for Studies and Projects (FINEP), in part by Araucaria Foundation, and in part by Federal University of Technology – Paraná (UTFPR)

(Corresponding author: Jean Carlos Cardozo da Silva) The authors are with the Graduate Program in Electrical and Computer Engineering, Federal University of Technology- Paraná, Curitiba 80230-901, Brazil (e-mail: ehdureck@gmail.com; daniel.benetti87@gmail.com; w_correia@live.com; thiagoh@utfpr.edu.br; hslopes@utfpr.edu.br; uiliandreyer@utfpr.edu.br; kleitonsousa@utfpr.edu.br; danielpipa@utfpr.edu. br; jeanccs@utfpr.edu.br).

operational states in low-voltage electromechanical relays and contactors. For instance, in Tapia et al. [2], the temperature and dynamic strain measurements on an electromagnetic AC contactor using FBG sensors were presented. Besides the no-fault condition, authors studied the dynamic strain measurement for three switching conditions of the contactor: with voltage sag, with an obstacle in the air gap, and without shading ring. The authors reported results in the frequency spectrum, indicating a peak of 120 Hz for the first two fault conditions and predominant components from 0 to 70 Hz range for the contactor without shading ring.

More specific works involving DC relays and FBGs include: Dureck *et al*. [13], and Benetti *et al*. [14] who proposed a real-time monitoring system for the switching conditions of a contactor. Different voltage loss conditions were applied to the equipment, and the system was capable of classifying the data with only two signal features, by using a Support Vector Machine (SVM). Other studies of similar applications for circuit breakers also showed that SVM is an interesting classification method for this purpose [15], [16]. To study the features of the signals of the switching event, the frequency spectrum is currently addressed based on the research cited above using FBGs [2], [13], [14] or other measurement systems such as electrical accelerometers in OLTCs [4]. Therefore, both Power Spectrum Density (PSD) and Fast Fourier Transform (FFT) are suitable to be used.

In Benetti *et al*. [17], different operating conditions were analyzed in the main internal components. We have applied two distinct methods: The first calculates the PSD components and the switching time, and the second obtains the wavelet scattering transform coefficients, showing that it is possible to detect normal and critical states with good reproducibility when using the same contactor and sensor for measurements.

In this paper, we introduce a real-time health monitoring system, specifically designed for AC contactors, with a strong emphasis on its wide generalization capability, particularly for field applications. Utilizing FBG sensors, chosen for their highlighted capabilities, and applying machine learning algorithms, this work aims to increase the generalization of the proposed diagnostic system to assist maintenance engineering in defect detection. One of the main advantages of the proposed analysis methods is the improvement in adaptability for measurements with a new contactor and assemblies.

To train the diagnostic system's machine learning, four operational state conditions were applied to the contactor. With the goal of ensuring the method's generalization, a test group was created, distinct from the training group, but maintaining the established standards. The proposed system was rigorously tested in a controlled environment, subjecting it to various conditions that faithfully replicate real-world field scenarios. Furthermore, a descriptive classification study was conducted with the explicit aim of deriving easily interpretable classification rules. These rules not only enhance the understanding of how contactor faults influence the frequency spectrum of the acquired signal but also highlight the practicality and potential for real-world deployment that the system offers.

This paper has been organized as follows. Section II presents the proposed methodology composed of the experimental setup of the contactor and the FBG sensor, including the acquisition of signal data. Next, feature extraction algorithms were used for those signals. Section III presents and discusses the results achieved in this paper. Finally, Section IV concludes the work by presenting the contributions and possible proposals for future research.

II. Materials and Methods

A. Experimental Setup

The tests were carried out with two AC contactors, model ABB AX40. The operation of this equipment consists of an electromechanical force generated by a coil connected to a 220V AC source. This force attracts the movable core to its fixed part, closing the load contacts. Since it is an AC contactor, shading rings are required to hold the core in position during the negative cycles of the current. When the source is off, the return spring brings the movable core to its original position opening the load contacts [18]. The mechanism of this contactor is better represented in Figure 1.

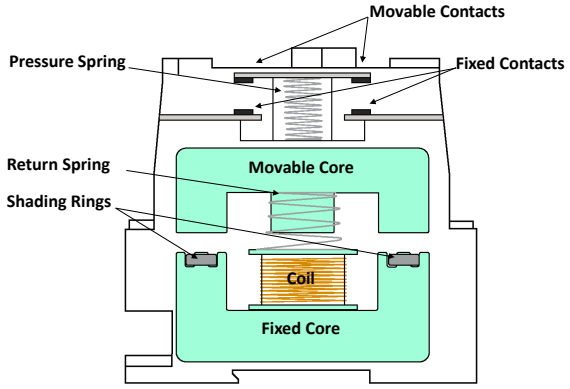

Fig. 1. Schematic representation of the ABB AX40 mechanism.

For both contactors, a pre-tensioned FBG was fixed to a cleaned region of the case by using a cyanoacrylate-based glue to capture the mechanical vibration of the closing contacts. Pre-tensioning enables the detection of compression and tension movements without damaging the FBG during the various assemblies required. The change in the central wavelength of the Bragg reflection in a Fiber Bragg Grating (FBG) can be described as (1):

$$\Delta\lambda_b = K_\epsilon \Delta_\epsilon + K_T \Delta_T \tag{1}$$

.

In (1), the Bragg wavelength shift ($\Delta\lambda_b$) is influenced by both the strain variation (Δ_ϵ) and the temperature change (Δ_T). The terms K_ϵ and K_T represent coefficients that account for these effects. The coefficient K_ϵ, known as the strain coefficient, has a typical value of around 1.2 pm/$\mu\epsilon$ in the 1.5 μm spectrum region, reflecting the relationship between strain and the resulting wavelength shift. Conversely, the coefficient K_T corresponds to the temperature coefficient, approximately 10 pm/K. This coefficient is derived from the thermal properties of the optical fiber used in the FBG setup

[19]. Additionally, while temperature variation occurs rapidly inside the contactor, it is much slower in the enclosure where the sensor is installed. Therefore, in terms of the propagation of mechanical waves, the temperature fluctuation is a relative slow event, in the order of tens of minutes, when compared to the mechanical waves propagating through solid materials, which are in the order of a couple of seconds. Also, the extracted features and the proposed algorithm is better optimized for vibration signals, consequently, the temperature influence on the Bragg wavelength variation is neglectable. The setup is presented in Figure 2.

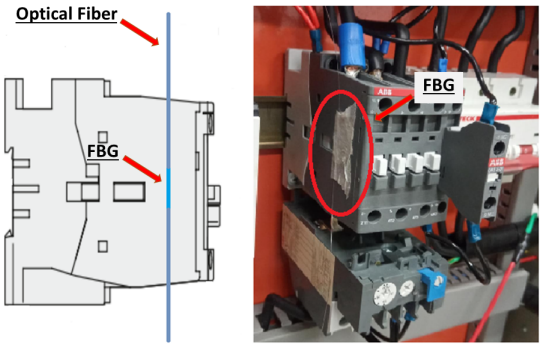

Fig. 2. Experimental setup for the experiments.

The optical fiber used was the GF1 Thorlabs type. Two FBGs were employed separately, one for each contactor. The first FBG had Bragg wavelength of 1552 nm, a reflectivity of approximately 95%, and a full-width at half maximum bandwidth of 0.5 nm. The other FBG had Bragg wavelength of 1532 nm, a reflectivity of approximately 80%, and a half-height bandwidth of 0.6 nm. To acquire the signals, the optical interrogator I-MON 256, by Ibsen Photonics, was used. The acquisition rate was set at 4kHz and 20 μs of exposure time. A sample of the wavelength variation by the vibration of the closing contacts with no fault applied is presented in Figure 3, the switching event is centered at the 0.5 second mark.

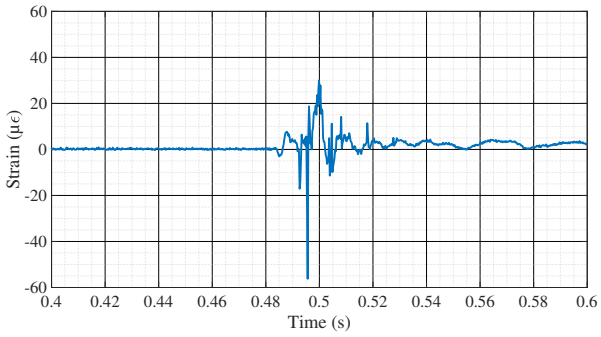

Fig. 3. Sample of the contactor with no fault measured by the FBG.

The accurate placement of FBG sensors is essential for precisely measuring the deformations caused by the dynamic excitation during the collision of moving parts against the static base structure of an AC contactor during its switching process. When the contactor closes, the kinetic energy of the moving parts is transformed into heat, noise, vibration, and deformation, until a stable closed state is reached [20], [21]. The FBG sensor was strategically placed on the contactor's surface to accurately capture the level of deformation experienced by the structure and be far from the heat point inside the device. This placement was based on expectations of maximum strain in the stationary base structure of the contactor, as indicated by the simulation of its first and second vibrational modes (Figure 4), conducted using Altair Software.

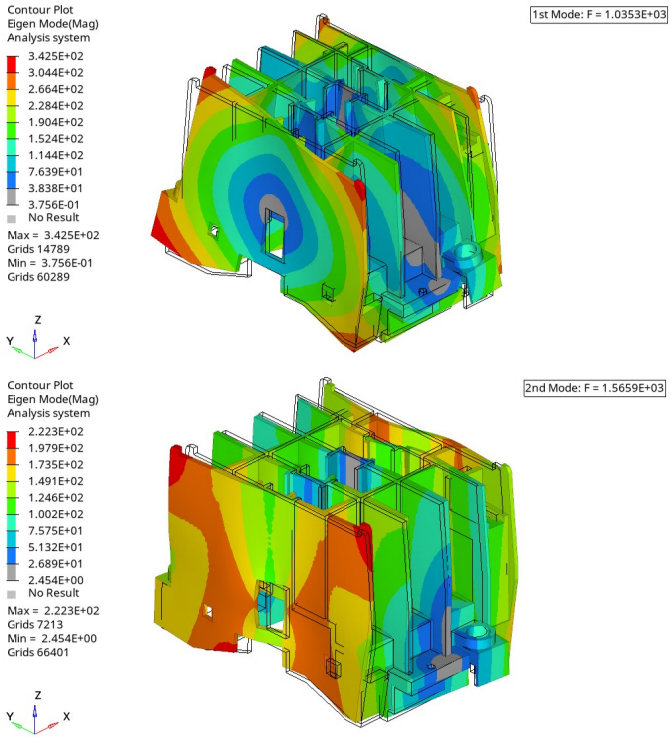

Fig. 4. Simulation of the firt and second vibrational mode of the ABB AX40 contactor given by strain energy density [kg/(mm·s^2)].

For this simulation, the mesh was created using Altair HyperWorks, and the analysis was performed with Altair Optistruct, with subsequent post-processing in Altair HyperView. The mesh comprised 423,900 tetrahedral CTETRA elements with a 1 mm size, ensuring quality with an aspect ratio greater than 5 and a skew angle less than 60 degrees. This setup was chosen after a mesh sensitivity analysis indicated that a 1 mm element size could capture deformations with less than 1% error in simulation results, a finding that was further validated by a comparative analysis using a finer 0.5 mm element, which only caused changes in the second decimal place of the results. The type of analysis conducted was a modal analysis. Additionally, when placing the FBG sensor

on the side of the AC contactor's structure, considerations were made for the ease of maintenance of both the sensor and the contactor, ensuring that the sensor's position did not interfere with the electrical wiring layout of the panel and the contactor's installation.

B. Datasets

The test procedure acquired 4 classes of data: 118 samples of the contactor at normal state (Class 0), 93 with pressure spring wear-off (Class 1), 93 with load contact wear-off (Class 2), and 80 with inner contact blockage (Class 3). All these samples were divided between the contactor (C1 or C2), being fixed or screwed to the electrical panel, and the test round (R1, R2, or R3). The variability of the FBG sensor, the contactor, fixation, and test round provide better generalization and repeatability for further analysis. Once all the data was acquired, the data set was split between train, testing, and validation. The train set is used to train the classifier, the validation set is used during training to evaluate the convergence and generality capability of the classifier, and the test set is used after training to evaluate the predictive quality of the classifier. Table I shows more details of the data sets.

TABLE I

DATA SET SHOWING THE NUMBER OF SAMPLES FOR EACH CLASS, CONTACTOR ($C = \{1, 2\}$) AND ROUND ($R = \{1, 2, 3\}$). THE DATA SET IS DIVIDED INTO TRAINING (UPPER TABLE), VALIDATION (LOWER TABLE, LEFT) AND TEST (LOWER TABLE, RIGHT).

	C1 R1 Fixed	C1 R2 Screwed	C2 R1 Screwed
Class 0	30 Samples	20 Samples	38 Samples
Class 1	30 Samples	20 Samples	13 Samples
Class 2	30 Samples	20 Samples	13 Samples
Class 3	30 Samples	20 Samples	N/A

	C1 R1 Fixed
Class 0	10 Samples
Class 1	10 Samples
Class 2	10 Samples
Class 3	10 Samples

	C1 R3 Screwed
Class 0	20 Samples
Class 1	20 Samples
Class 2	20 Samples
Class 3	20 Samples

The disparity in data group sizes does not impact the outcomes, thanks to the effective evaluative metric employed. Moreover, the limited data for Class 3 is a consequence of its significant difference observed in comparison to other classes, hence there is no need for large quantities of data for something highly distinguishable.

Actually, the original training data set was quite small. This was due to the difficulty in applying the faults and acquiring the data. In order to circumvent such limitations, we used a data-augmentation procedure. Data-augmentation consists in including specific small transformations to the input data (including several types of noise), in order to create diversity and make the classifier more robust. Such a procedure has been proved to increase the classifier's efficiency in many scenarios [22].

For data-augmentation, the original 264 training signals were submitted to a procedure for synthesizing more data. First, another 264 signals were generated, using variable noise and gain, and a small chance of hyperbolic tangent and pitch distortion. Next, 264 more signals were generated, now with higher variable noise, linear growth, and also a small chance of distortion. This linear growth simulates external temperature variation. Therefore, a total of 792 signals were used as training data.

The data set was divided into three root classes, as follows: Main Class 0 is the no-fault class, Main Class 1 is the mild fault class, composed of the classes of worn springs and worn contacts, and Main Class 2 is the serious fault class, composed by the core blockage class. If a mild fault is identified, a binary classification within the light faults must be made to find out if the cause is contact or spring wear-off. This type of analysis by layers allows the activation of maintenance teams even in cases of inaccuracies about the exact class of fault designated.

C. Feature Extraction and Classification Algorithms

All the signals, both original and augmented, were submitted to two feature extraction algorithms. The first one includes power and spectral features by using PSD combined with FFT. The signals were normalized and processed, after that, for each 50 Hz of a sliding window, the mean value of the PSD and the maximum value of the FFT were extracted, generating 80 features. For this procedure, we used MATLAB version R2020b software.

The other feature extraction algorithm used was the Time Series Feature Extraction Library (TSFEL) [23]. This is a Python library capable of computing over 60 different types of features extracted from temporal, statistical, and spectral domains. It aims to support a fast exploratory analysis, and it has already been used in data sets from wearable accelerometer sensors for human activity recognition. For our data set, a total of 390 features were extracted from each signal.

Since many features were generated from the signals and, possibly, many of them may not be useful for the classification algorithm, the next step is a feature selection procedure. The goal here is to select the most discriminatory features so as to improve the classification rate.

There are two families of methods for feature selection: filter and wrapper methods. Filter methods are fast and easy since they select a number of features based on some user-defined criteria [24]. In this work, the Best ReliefF Ratio (BRR) criterion was chosen using the Orange software [25].

Another used filter method was based on the Physical Analysis (PA) of the signals and the contactor construction. This is an analysis that takes advantage of all PSD and FFT features subjected to classifiers based on decision rules to obtain human-comprehensible interpretability of the switching event, this being a reason why the PA did not address aspects of the TSFEL. This is a more subjective filter method based on interpreting the physical importance of the studied frequencies.

Regarding the wrapper methods, they use a classifier to test a given subset of features, which, in turn, are selected from the original set. Despite being more computationally expensive, wrapper methods usually obtain better results than filter methods [26]. In this paper, we used the Sequential

Forward Floating Selection (SFFS) method, which is a tool based on the Sequential Forward Selection (SFS), correcting wrong decisions made in the previous steps to optimize the solution [27].

For all the feature selection algorithms used in this paper, the SVM classifier, using the Radial Basis Function Kernel function (RBF) and cross-validation of 10 folds, is proposed. The SVM is a robust algorithm used for classification and regression tasks. Its primary objective is to distinguish between different classes in a dataset by finding the optimal hyperplane that maximizes the margin, or separation distance, between these classes [28]. This margin is defined by the distance between the nearest points (support vectors) of different classes that lie along the hyperplane's boundaries. The RBF Kernel function is given by (2):

$$K_{RBF}(X_i, X_j) = e^{\left(-\frac{\|X_i - X_j\|^2}{2\sigma^2}\right)}, \tag{2}$$

where the relation between X_i and X_j represents the Euclidean distance of two data points. This distance is inversely related to σ^2, the variance, which is a crucial hyper-parameter in the model [29]. Importantly, hyper-parameters like σ in the RBF Kernel can be fine-tuned to better suit the training and validation groups, enhancing the model's performance. This tuning process involves adjusting these parameters to find the best balance between bias and variance, thereby improving the classifier's ability to generalize from the training data to unseen data.

For algorithm evaluation, cross-validation is crucial. It splits the training dataset into several smaller subsets or folds, ensuring a more robust and generalized performance from the classifier. Given the imbalance in our dataset, the F1 score is preferred over accuracy for evaluating the three Main Classes. The F1 score is more effective in contexts with uneven class distributions, as it provides a balanced measure of precision and recall. However, for the balanced mild fault classes, accuracy is a suitable metric due to the uniform distribution of samples across these classes.

Regarding the usage of PA, 12 main features were identified to define the 3 Main Classes, achieving an F1 macro score of 0.738 for the training data set. As for the training group of 2 mild fault classes, only 4 main features were used, and it achieved an accuracy of 0.802. The study to obtain such attributes was mainly based on the CN2 Rule (CN2R) and Decision Tree (DT) classifiers using all PSD and FFT attributes with the intention of extracting logical rules to know how the faults occurring in the contactor affect the frequency spectrum of the acquired signal. It is important to note that the main classifier is still the SVM due to better results in general with previous sampling tests.

The CN2R works by selecting the most informative features in the data set and creating rules based on those attributes with the corresponding value of the output variable. Once a rule has been created, the algorithm removes the data that satisfy the rule from the data set, and the process is repeated on the remaining data until a stopping condition is achieved. Regarding DT, it works by recursively partitioning the data set into subsets based on the values of the input features. At each decision node, the algorithm selects the best attribute to split the data set based on a certain criterion, such as ReliefF. The feature that maximizes the criterion is chosen to split the data set into two or more subsets, in this paper, we used two. This process is repeated on each subset until a stopping criterion is achieved.

Using the mild fault classes as an example, in order to better understand how this method works, a critical analysis can be made based on the most influential rules of the CN2R as shown in Table II and the first four layers of the DT presented in Figure 5.

TABLE II
MOST INFLUENTIAL RULES OF THE MILD FAULT CLASSES.

IF Condition	Class 1	Class 2
TRUE	189	189
PSD4 ≤ -88.9 AND PSD16 ≥ -98.8	69	0
PSD5 ≥ -81.5 AND PSD3 ≥ -79.3	0	45
PSD5 ≥ -82.3	0	43
PSD1 ≥ -74.5	34	0
PSD5 ≥ -81.5 AND PSD4 ≥ -76.4	0	27
PSD1 ≥ -77.9	20	0
PSD2 ≤ -83.3 AND PSD20 ≥ -102.6	16	0

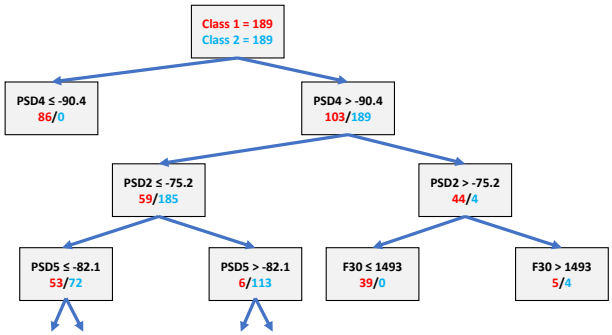

Fig. 5. First four layers of the decision tree of the mild fault classes.

One can see a PSD variation from 0 to 250 Hz (PSD1 to PSD5) and 1000 to 1050 Hz (PSD20), indicating that the difference between the two event signals occurs mainly in these frequency ranges. In addition, an analysis of the distribution of frequency peaks by the FFT shows a shift of the peak frequency of 60 Hz, characteristic of a healthy contactor (F2), indicating a possible contact bounce for worn contact cases. This implies at least seven potential features to be used with the RBF SVM to classify mild faults.

Regarding BRR and SFFS, to choose the ideal number of features, it is necessary to make a relationship between the training success metric and the percentage of total features used. The percentage of total attributes and the metric scores using RBF SVM by features extractor and selector are presented in Figure 6 and Figure 7.

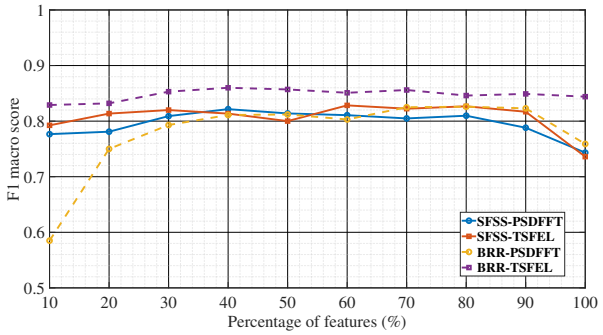

Fig. 6. F1 macro scores of the training data set of the 3 Main Classes using both feature selection methods.

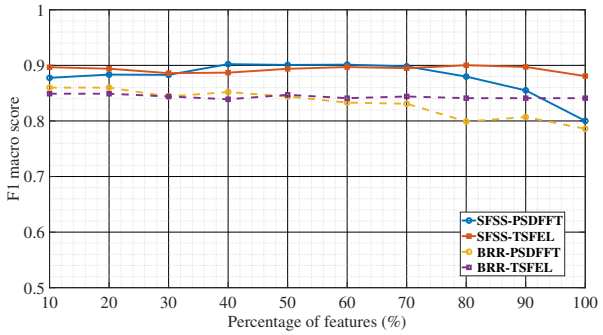

Fig. 7. Accuracy scores of the training data set of the two mild fault classes using both feature selection methods.

One can observe the similarity of the results from both feature selection methods and feature extractor algorithms. From the graphs presented, it is evident that the first graph shows good metric stability with 30% to 80% of the features for the SFFS. However, the use of 30% of the features significantly reduces the computational load when applying machine learning algorithms. As for the second graph, the SFFS method remains relatively stable throughout its course. Nonetheless, for standardization purposes and considering that the computational burden remains low, maintaining 30% of the features was deemed appropriate in all cases of SFFS. This ensures a balance between efficiency and effectiveness in the feature selection process. As for BRR, the ideal percentage remains 30% for the second layer of the classifier, however in the first layer it was necessary to use 40% of the features.

III. Results and Discussions

After choosing the number of features among the five options presented for each layer of the classifier, fine-tuning the hyperparameters of the SVM was implemented to achieve the best possible results in the training and validation data set. The preliminary results are presented in Figure 8 and Figure 9.

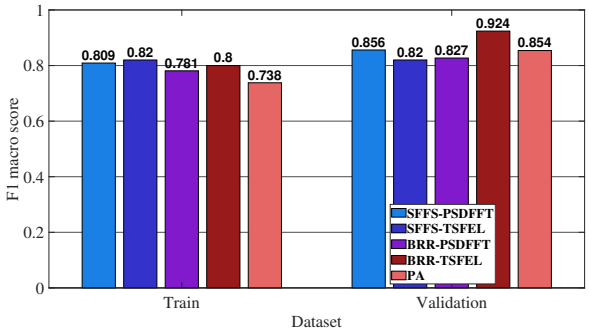

Fig. 8. F1 macro scores of the training and validation data set of the three Main Classes.

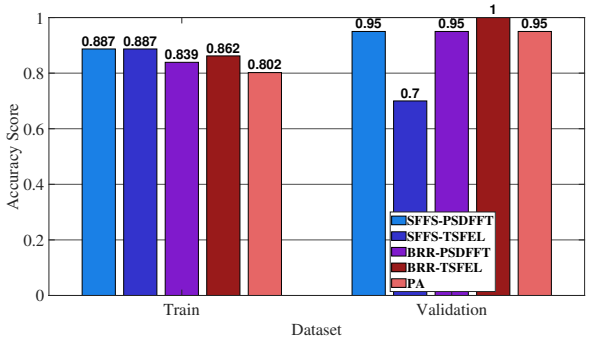

Fig. 9. Accuracy scores of the training and validation data set of the mild fault classes.

Based on the findings presented in the training and validation groups, all methods demonstrate potential for application, as evidenced by the high and comparable scores for both classifications. Regarding the classification of mild faults, the outcomes were superior, suggesting that the algorithms may have greater proficiency in distinguishing between two minor faults than in differentiating between the no-fault class and the mild faults class. However, as shown in Figure 10, when the classifier is applied to the repeatability test group, the metric values have considerable inconsistency.

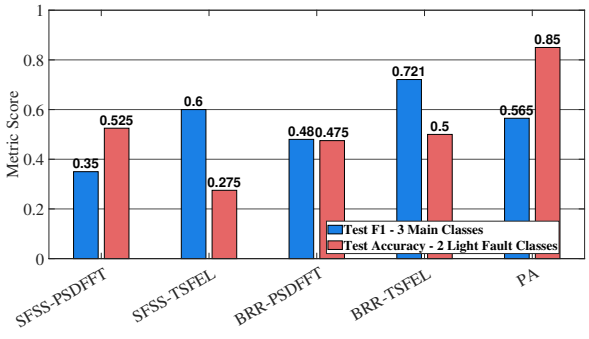

Fig. 10. Metric scores of the repeatability test.

Therefore, for the layer of three Main Classes of the SVM, the usage of TSFEL together with BRR proved to be viable with a better generalization and less overfit. However, the results of the class without faults and the class with mild defects still have some overlap due to the small degree of

the applied conditions. This can be deducted by the confusion matrix of the training data set in Figure 11.

		Predicted			
Class		0	1	2	∑
Actual	0	190	72	2	264
	1	77	297	4	378
	2	2	4	144	150
∑		269	373	150	792

Fig. 11. Confusion matrix of the training data set using 3 Main Classes.

Nevertheless, the algorithm fulfills its purpose of alerting teams to severe and minor faults. Regarding the second layer of the algorithm, the differentiation of just two classes proves more promising with a physical analysis of the switching event. Therefore, the identification of the light fault is given by PA with features of PSD and FFT.

Furthermore, PA can help identify factors such as a peak frequency at 120Hz due to contact bounce during switching attempts and a higher spectral density at low frequencies, noticeable in the core blockage class. The other three original classes were more challenging to define, with notable subtle changes involving the PSD ranges between 0 and 250 Hz, 750 and 850 Hz, and 1000 and 1250 Hz. Other factors, such as a shift in the lower peak frequencies with the worn contact class, are of interest as they may indicate a contact bounce, as previously reported. By isolating the classes of slightly worn springs and contacts, the difference in the mentioned frequency bands is more noticeable, being able to differentiate these subtle events more clearly than BRR and SFFS.

The variations in PSD amplitude and frequency shift identified by the PSD and FFT method suggest a change in the deformation of the contactor base structure acquired by the FBG sensor for each failure class when compared to the contactor at a normal state. A more significant change in deformation and higher strain rates was noticeable in the core blockage class because BRR and SFFS easily identified it. Mild faults were better captured using PA, which implies minor deformation changes and lower strain rates than those generated by the core blockage class.

The final results of the developed contactor fault classification algorithm are presented in Figure 12.

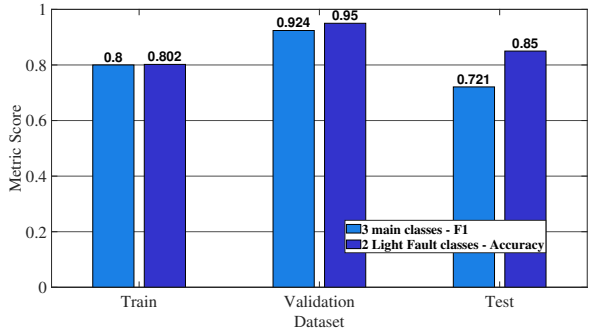

Fig. 12. Metric scores of the pattern recognition system

This system presents reliability above 80% for training and validation of the two layers of the SVM classifier. It is also observed that the study of features and the combination of multiple attributes extractors and selectors using different physical parameters allowed a better test repeatability. Hence, the results obtained with the test data set do not present a significant overfit of the classifier, achieving scores above 70%.

Unlike our earlier studies [17] and those by Tahvilzadeh *et al* [30], this research focuses on a pragmatic and tangible methodology for fault detection in electrical switching devices. However, conducting a direct numerical comparison with these studies is impractical due to differences in datasets. Our older dataset lacks the variability necessary for broader generalization and applicability in diverse test scenarios [17].

In our current approach, we emphasize a broader range of case variabilities, incorporating data from various assemblies and contactors. Key to our methodology are the data augmentation technique and feature selection via attribute analysis. These are pivotal in practical scenarios where repetitive invasive data collection is often not viable, and the inherent random variabilities within the system pose a challenge to comprehend.

While our accuracy is somewhat low, this approach allows for better generalization and adaptation to the variable complexities of real-world signal acquisition in electrical environments.The accuracy might possibly be enhanced by incorporating a greater diversity of data and additional decision layers. However, there is always a limit to this enhancement to avoid overfitting and compromising the model's ability to generalize. Furthermore, our study also focuses on extracting meaningful physical information from the contactor's classification attributes, contributing to a deeper understanding of the fault detection process. Therefore, our research offers a practical and valuable perspective on applying FBG technology for detecting faults in electrical contactors in real-world environments. In such a scenario, accuracy may be strongly influenced by various challenging variables.

FBGs also proved to be reliable sensors for monitoring systems. Using only one external sensor, it was possible to achieve relevant results, with room for improvement in future invasive applications.

IV. Conclusions

This paper complements previous studies on the viability of a machine learning system using FBG as a sensor element to determine the operating conditions of switching equipment. Filter methods for attribute selection and feature extraction via PSD and FFT proved to be a reliable source of information to understand the physics of the contactor and optimize the pattern recognition system. Also, the procedure led to a similar performance of the commonly used feature extractor TSFEL. The results between training, validation, and repeatability test data sets are well balanced with minor classification overfit despite some overlapping data due to the light grade of the faults.

The repeatability study was important for future field applications since minor physical variations will eventually happen. The developed system proved to be effective using SVM

as a classifier and a single FBG as a sensor element. This research also has the potential to be expanded to an invasive monitoring system in other switching equipment due to the sensor characteristics. The sensitivity between different stages of degradation will be evaluated for an anomaly detection system. The usage of other methods, such as Empirical Mode Decomposition or Hilbert Spectrum will be focused on future works.

REFERENCES

[1] W. Rieder and T. W. Strof, "Reliability of commercial relays during life tests at low electrical contact load," *IEEE Transactions on Components, Hybrids, and Manufacturing Technology*, vol. 15, no. 2, pp. 166–171, 1992.

[2] C. C. Tapia, J. L. R. Ortiz, U. J. Dreyer, J. C. C. da Silva, and K. de Morais Sousa, "Evaluation electromagnetic contactor magnetic core temperature and dynamic strain using fiber Bragg gratings," *Measurement*, vol. 166, p. 108174, 2020.

[3] A. I. Khalyasmaa, M. D. Senyuk, and S. A. Eroshenko, "High-voltage circuit breakers technical state patterns recognition based on machine learning methods," *IEEE Transactions on Power Delivery*, vol. 34, no. 4, pp. 1747–1756, 2019.

[4] A. Cichoń, T. Boczar, P. Fracz, and D. Zmarzły, "Detection of defects in on-load tap-changers using acoustic emission method," in *Proc. International Symposium on Electrical Insulation*. IEEE, 2012, pp. 184–188.

[5] J. Seo, H. Ma, and T. K. Saha, "Analysis of vibration signal for power transformer on-load tap changer (OLTC) condition monitoring," in *Proc. Power & Energy Society General Meeting*. IEEE, 2018, pp. 1–5.

[6] H. Hoidalen, M. Runde, O. Haugland, G. Ottesen, and M. Ohlen, "Continuous monitoring of circuit-breakers using vibration analysis," in *Proc.* 11^{th} *International Symposium on High Voltage Engineering*, vol. 1. IET, 1999, pp. 102–106.

[7] R. Min, Z. Liu, L. Pereira, C. Yang, Q. Sui, and C. Marques, "Optical fiber sensing for marine environment and marine structural health monitoring: A review," *Optics & Laser Technology*, vol. 140, p. 107082, 2021.

[8] J. de Pelegrin, U. J. Dreyer, C. Martelli, and J. C. C. da Silva, "Optical fiber sensor encapsulated in carbon fiber reinforced polymer for fault detection in rotating electrical machines," *IEEE Sensors Journal*, vol. 20, no. 19, pp. 11 364–11 371, 2020.

[9] A. Mohammed, J. I. Melecio, and S. Djurović, "Stator winding fault thermal signature monitoring and analysis by *in situ* FBG sensors," *IEEE Transactions on Industrial Electronics*, vol. 66, no. 10, pp. 8082–8092, 2018.

[10] A. Othonos and K. Kalli, *Fiber Bragg Gratings Fundamentals and Applications in Telecommunication and Sensing*. Artech House Publishers, 1999.

[11] R. Kashyap, *Fiber Bragg gratings*. Academic Press, 1999.

[12] F. Marignetti, E. de Santis, S. Avino, G. Tomassi, A. Giorgini, P. Malara, P. De Natale, and G. Gagliardi, "Fiber Bragg grating sensor for electric field measurement in the end windings of high-voltage electric machines," *IEEE Transactions on Industrial Electronics*, vol. 63, no. 5, pp. 2796–2802, 2016.

[13] E. H. Dureck, D. Benetti, U. J. Dreyer, and J. C. C. da Silva, "Fault analysis in electromechanical relays's switching using fiber Bragg grating," in *Proc. of SBMO/IEEE MTT-S International Microwave and Optoelectronics Conference*. IEEE, 2021, pp. 1–3.

[14] D. Benetti, E. H. Dureck, U. J. Dreyer, A. E. Lazzaretti, D. R. Pipa, and J. C. C. da Silva, "Classification dynamic strain patterns in switching devices measured with fiber Bragg grating," in *Proc. of SBMO/IEEE MTT-S International Microwave and Optoelectronics Conference*. IEEE, 2021, pp. 1–3.

[15] J. Huang, X. Hu, and F. Yang, "Support vector machine with genetic algorithm for machinery fault diagnosis of high voltage circuit breaker," *Measurement*, vol. 44, no. 6, pp. 1018–1027, 2011.

[16] Y. Kai and L. Jian, "Rcm scheduling optimization for circuit breakers based on ls-svm," in *Proc. of International Conference on Connected Vehicles and Expo*. IEEE, 2014, pp. 162–169.

[17] D. Benetti, E. H. Dureck, U. J. Dreyer, D. R. Pipa, and J. C. C. Da Silva, "Feature extraction and selection for identifying faults in contactors using fiber bragg grating," *IEEE Sensors Journal*, 2023.

[18] J.-R. R. Ruiz, A. G. Espinosa, and L. Romeral, "A computer model for teaching the dynamic behavior of ac contactors," *IEEE Transactions on Education*, vol. 53, no. 2, pp. 248–256, 2009.

[19] P. Zhu, J. Wu, M. Huang, Y. Wang, P. Liu, and M. A. Soto, "Reducing residual strain in fiber bragg grating temperature sensors embedded in carbon fiber reinforced polymers," *Journal of Lightwave Technology*, vol. 37, no. 18, pp. 4650–4656, 2019.

[20] S.-Y. Lin and X.-S. Huang, "Full simulation of ac contactor in the dynamic process based on finite element method," *Journal of Information Hiding and Multimedia Signal Processing*, vol. 7, pp. 781–790, 01 2016.

[21] G. Zhang, W. Chen, C. Ke, P. Zheng, and Y. Geng, "Full simulation of ac contactor in the dynamic process based on finite element method," *Simulation and optimization of dynamic characteristics of intelligent AC contactor*, vol. 33, pp. 225–233, 10 2010.

[22] N. M. R. Aquino, M. Gutoski, L. T. Hattori, and H. S. Lopes, "The effect of data augmentation on the performance of convolutional neural networks," in *Proc. XIII Brazilian Congress on Computational Intelligence*. SBIC, 2017, pp. 1–12.

[23] M. Barandas, D. Folgado, L. Fernandes, S. Santos, M. Abreu, P. Bota, H. Liu, T. Schultz, and H. Gamboa, "TSFEL: Time series feature extraction library," *SoftwareX*, vol. 11, p. 100456, 2020.

[24] S. Mishra, P. Chaudhury, B. K. Mishra, and H. K. Tripathy, "An implementation of feature ranking using machine learning techniques for diabetes disease prediction," in *Proc. of the* 2^{nd} *International Conference on Information and Communication Technology for Competitive Strategies*, 2016, pp. 1–3.

[25] J. Demšar, T. Curk, A. Erjavec, Črt Gorup, T. Hočevar, M. Milutinovič, M. Možina, M. Polajnar, M. Toplak, A. Starič, M. Štajdohar, L. Umek, L. Žagar, J. Žbontar, M. Žitnik, and B. Zupan, "Orange: Data mining toolbox in python," *Journal of Machine Learning Research*, vol. 14, pp. 2349–2353, 2013.

[26] B. Li and M. Q.-H. Meng, "Tumor recognition in wireless capsule endoscopy images using textural features and svm-based feature selection," *IEEE Transactions on Information Technology in Biomedicine*, vol. 16, no. 3, pp. 323–329, 2012.

[27] P. Pudil, J. Novovičová, and J. Kittler, "Floating search methods in feature selection," *Pattern Recognition Letters*, vol. 15, no. 11, pp. 1119–1125, 1994.

[28] W. Miao, Q. Xu, K. Lam, P. W. Pong, and H. V. Poor, "Dc arc-fault detection based on empirical mode decomposition of arc signatures and support vector machine," *IEEE Sensors Journal*, vol. 21, no. 5, pp. 7024–7033, 2020.

[29] G. O. Anyanwu, C. I. Nwakanma, J.-M. Lee, and D.-S. Kim, "Optimization of rbf-svm kernel using grid search algorithm for ddos attack detection in sdn-based vanet," *IEEE Internet of Things Journal*, 2022.

[30] M. Tahvilzadeh, M. Aliyari-Shoorehdeli, and A. A. Razi-Kazemi, "Model-aided approach for intelligent fault detection system for sf 6 high-voltage circuit breaker with spring operating mechanism," *IEEE Transactions on Power Delivery*, 2023.